Journal of the European Ceramic Society 22 (2002) 121–128

www.elsevier.com/locate/jeurceramsoc

(Crack-healing + proof test): a new methodology to guarantee the structural integrity of a ceramics component

K. Ando [a,*], Y. Shirai [a], M. Nakatani [b], Y. Kobayashi [b], S. Sato [b]

[a] *Department of Energy and Safety Engineering, Yokohama National University, 79-5, Hodogaya, Yokohama, Japan*
[b] *NHK Spring Co. Ltd., 3-10 Fukuura, Kanazawaku, Yokohama, Japan*

Received 19 October 2000; received in revised form 2 February 2001; accepted 16 February 2001

Abstract

Structural ceramics are brittle and sensitive to flaws. As a result, the structural integrity of a ceramic component may be seriously affected. To overcome this problem, there are three ways: (a) inspect carefully and repair the unacceptable flaws, (b) toughen the ceramics by fiber reinforcing, (c) heal the flaws and recover strength. At the moment, there is no technique to heal embedded flaws. Therefore, a new technique to guarantee the reliability of ceramics components is demanded and so we proposed new technique: (crack-healing + proof test). For this technique, the mechanical behaviour of the crack-healed zone is very important for the structural integrity. Bending strength and fatigue strength test results of the crack-healed zone at high temperature are described. Using a process zone size failure criterion, an equation for the temperature-dependence of proof stress (σ_P^T) is derived. The accuracy of the equation has been verified for monotonic loading tests up to 1300°C.

Keywords: Crack-healing; Mechanical Properties; Proof test; Si_3N_4; Test methods

1. Introduction

Generally speaking, structural ceramics are superior in strength than metal at high temperature. However, they are brittle and sensitive to flaws. As a result, the structural integrity of a ceramics component may be seriously affected. To overcome this problem, there are three ways: (a) inspect carefully and repair the unacceptable flaws, (b) toughen the ceramics by fiber reinforcing, (c) heal the flaws and recover strength. For method (a), allowable flaws in ceramics are so small that it is almost impossible to detect the flaws. Moreover, structural ceramics are so brittle that repair is almost impossible. For method (b), many studies have been made around the world. However, very few studies have been made of method (c). Some engineering ceramics have the ability to heal a crack.[1–22] If this ability is used on structural components in engineering use, considerable advantages can be anticipated in the following fields:[12,17] (1) increases in the reliability of structural ceramic components; (2) decreases in the machining and inspection costs of ceramic components; and (3) decreases in the maintenance costs and prolongation of the lifetime of ceramic components.

From the above points of view, systematic study of the following items are desired: (i) a method to evaluate a crack-healing ability of a material,[5,10,12,17] (ii) effect of chemical compositions on the crack-healing ability of ceramics,[11,14,16] (iii) effect of healing condition on the mechanical behaviours of crack-healed zone,[10–12,14–17,19] (iv) maximum crack size which can be healed completely,[12,14,22] (v) high temperature strength of crack-healed member,[10,12,14,17,19] (vi) cyclic and static fatigue strength of crack-healed member at high temperature,[15,17–22] (vii) crack-healing behaviour under static or cyclic loading and crack-healing potential.[17,20,21]

The ceramics developed by authors which show excellent crack-healing ability are Si_3N_4/SiC[10] and mullite/SiC[14] composite ceramics. The crack-healing behaviours of both ceramics have been studied systematically. Most of these specimens failed outside the crack-healed zone even for a fatigue test using a three-point bending load,[15,17,18,22] these specimens have a Vickers indentation which acts as a stress concentration. Then, it can be concluded that the crack-healed zone of the Si_3N_4/SiC has higher bending strength and fatigue strength than

* Corresponding author.
E-mail address: andokoto@ynu.ac.jp (K. Ando).

0955-2219/01/$ - see front matter
PII: S0955-2219(01)00236-9

that of a base material up to 1300°C,[10,12,17,20,22] and 1200°C, [20,22] respectively. However, embedded cracks and micro-structural flaws such as abnormally large grains cannot be healed. This fact was confirmed many times by examining the crack initiation sites using SEM.[12,14–22] These facts suggest the importance of a proof test for higher reliability. There are many useful researches on a proof tests for a ceramics component[23–27] based on linear fracture mechanics, and on a probabilistic fatigue S–N curve which can be guaranteed by a proof test.[28–30] However, engineering ceramics show non-linear fracture behavior, as shown in Fig. 5. Therefore, a new theory is required, which is related to the proof test and based on non-linear fracture mechanics. Moreover, ceramics components are not used only at proof-tested temperature. Thus, a theory to explain the temperature dependence of proof stress based on non-linear fracture mechanics is necessary. From the above point of view, recently we proposed the new method, that is (crack-healing + proof test).[31] However, the usefulness was not yet proved. It is a purpose of this paper to prove the usefulness of (crack-healing + proof test).

In this paper, firstly, the usefulness of the technology (crack-healing + proof test) is considered, using high temperature and fatigue strength data of the crack-healed zone. Secondly, the equation which describes the effect of temperature on proof stress (σ_P^T) is derived. Finally, using a sintered rod made of silicon nitride specimen, the accuracy of the equation is confirmed.

2. Theory

2.1. Fracture and fatigue strength of crack-healed member at high temperature

For the technique (crack-healing + proof test), the mechanical behaviour of crack-healed ceramics members is very important because, firstly, crack-healing is made to avoid a fracture from surface flaws such as grinding cracks. In Figs. 1–3, the temperature dependence of the bending strength and fatigue strength of the crack-healed Si_3N_4 members are shown.[12,16] Material A is Si_3N_4 with SiC 20 vol.%, Y_2O_3 5 wt.% and Al_2O_3 3 wt.%. Material B is also Si_3N_4 with SiC 20 vol.% and Y_2O_3 8 wt.%. Material A (in Figs. 1 and Fig. 2) and material B (in Figs. 1 and 3) were both hot pressed and not proof-tested and material A in Figs. 1 and 3 are different batches. Then, bending strength at room temperature of both samples showed a little different value. The crack-healed member of silicon nitride A showed the almost constant bending strength up to 1000°C. However, above 1000°C, bending strength decreased with increasing testing temperature. In contrast, the crack-healed member of silicon nitride B showed the almost same bending strength up to 1400°C.

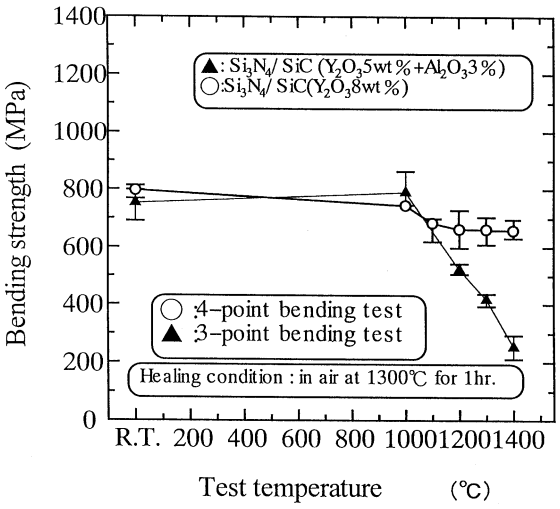

Fig. 1. Effect of test temperature on the bending strength of crack-healed specimen.

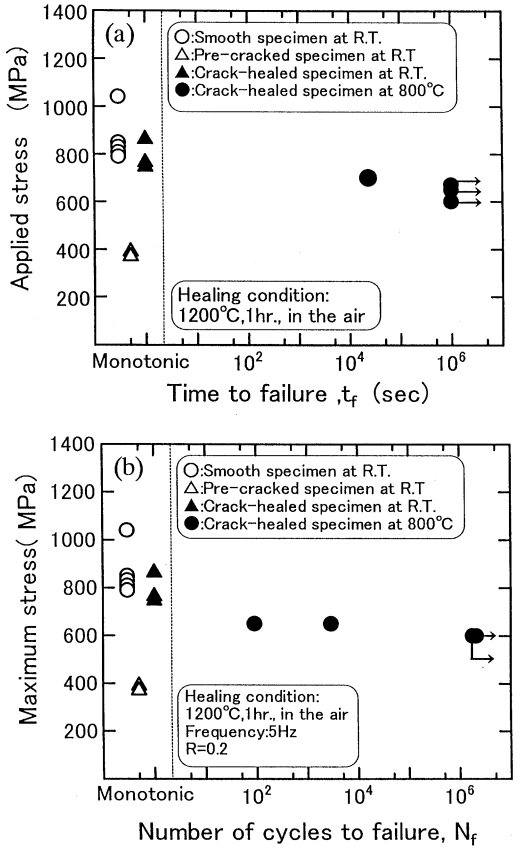

Fig. 2. Cyclic and static fatigue strength of crack-healed Si_3N_4(A) specimen at 800°C.

In Fig. 2, the cyclic and static fatigue strength of crack-healed Si_3N_4 (A) is shown.[18,22] From this figure, cyclic and static fatigue limit at $N_f = 2\times10^6$ cycles or $t_f = 10^6$ s are given as 600 and 650 MPa, respectively. These values are just a little lower than the bending strength of the smooth specimen at room temperature. However, the crack-healed zone is very weak at 1000°C, [18] and the

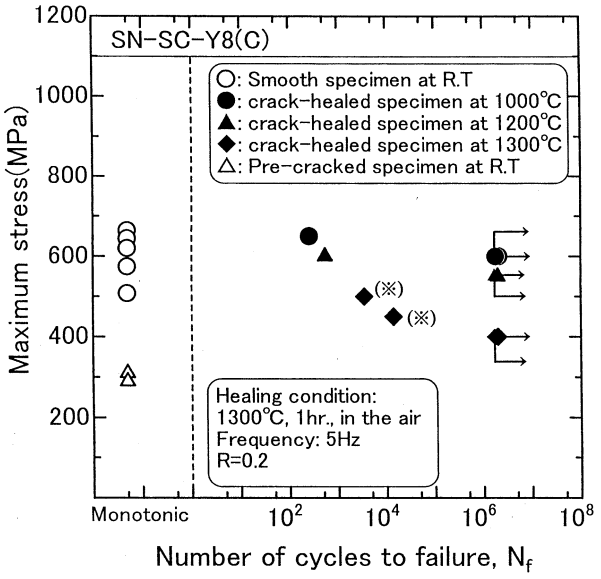

Fig. 3. Effect of test temperature on the cyclic fatigue strength of crack-healed Si_3N_4(B) specimen at high temperature range.

static fatigue limit is only 300 MPa. In Fig. 3, the temperature dependence of cyclic fatigue strength in silicon nitride B is shown.[22] From this figure, it can be seen that the crack-healed member has same cyclic fatigue limit at 1000 and 1200°C, and the value is almost the same as the bending strength of the smooth specimen at room temperature. Moreover, in Fig. 1 (sample A: below 1000°C, sample B: below 1300°C) and in Fig. 2, most samples fracture outside the crack-healed zone.[12,17,18] The healed zone is very narrow. Then if fracture occurred outside the crack-healed zone, it can be concluded that the healed zone has higher strength than the base material. From the above facts, it can be concluded that the crack-healed member has the same level strength as the base material. Then, it can be concluded that crack-healing is a very useful technique for the structural integrity of the ceramics member.

The estimated crack-healing reactions of the silicon nitride A and B are:[10,12,14]

$$Si_3N_4 + 3O_2 = 3SiO_2 + 2N_2$$

$$SiC + 2O_2 = SiO_2 + CO_2$$

$$2SiC + Y_2O_3 + 4O_2 = Si_2Y_2O_7 + 2CO_2$$

Silicon nitride A and B cannot heal a crack in a nitrogen or argon gas environment or in a vacuum condition,[10,12] however, it can heal a crack in an air environment. From these facts, most oxygen for healing reaction is assumed to come from air. It was observed that fracture initiated from embedded flaws in many crack-healed samples and, also, many embedded flaws were observed on the fracture surface.[12,14–22] From these facts, it can be concluded that embedded flaws can be healed hardly. Consequently, for higher reliability, a proof test is necessary even for the crack-healed element.

2.2. Temperature dependence of proof stress

In most ceramics, a process zone is developed ahead of the crack tip, as shown in Fig. 4. In this process zone, innumerable micro-cracks occur, or the volume increases as a result of phase transformation induced by stress.[32] Therefore, the stress in the area decreases to the level of process zone forming stress σ_0, and ceases to show the $1/\sqrt{r}$ singularity. The stress distribution in the process zone is sometimes thought to evolve characteristics due to work hardening or softening materials similar to AO or CO, respectively, in Fig. 4.[32] This process zone is quite similar to the yield zone of metals. This paper assumes for simplicity, however, that the stress σ_0 is constant, i.e. BO in Fig. 4.

When the process zone size D is small compared with both crack length and ligament width, D is expressed by Eq. (1) using the stress intensity factor K and σ_0.

$$D = \pi/8 \cdot (K/\sigma_0)^2 \tag{1}$$

However, when D is relatively large in comparison with the crack length, D is expressed by Eq. (2) using the Dugdale[33] model.

$$D = a_e\,[\sec(\pi\sigma/2\sigma_0) - 1] \tag{2}$$

Assuming that fracture occurs when the process zone size D reaches a certain limit, the fracture condition can be expressed as $D = D_C$. This is a process zone size failure criterion.[34–36] Therefore, the relationship between the fracture stress σ_C of a cracked sample and the equivalent crack length a_e can be expressed as follows:[34–36]

$$\frac{\pi}{8}\left\{\frac{K_{1c}}{\sigma_0}\right\}^2 = a_e\left\{\sec\left(\frac{\pi\sigma_c}{2\sigma_0}\right) - 1\right\} \tag{3}$$

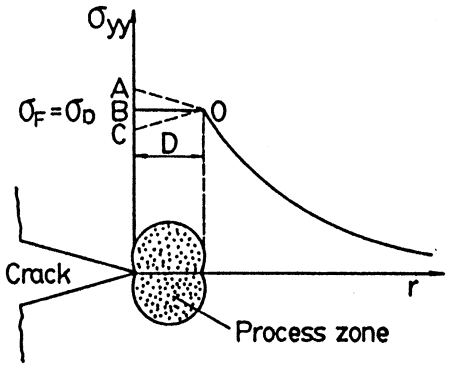

Fig. 4. Process zone ahead of crack tip and stress distribution.

where K_{1C} is plane strain fracture toughness, $\sigma_C = K_{1C}(\pi a_e)^{-1/2}$ and σ_0 is the process zone forming stress and is equal to the fracture stress of the plain specimen.[34–36]

The relationship between fracture stress σ_C and the equivalent crack length a_e is shown in Fig. 5.[34] The broken line and full lines show the relationship between σ_C and a_e based on K_{1C} and the process zone size failure criterion, respectively. The experimental relationship between σ_C and a_e in the 0.001∼0.2 mm range agrees very well with Eq. (1). It is shown that Eq. (3) based on the process zone size failure criterion shows good agreement with experimental data for Si_3N_4, SiC, Al_2O_3 and sialon.[34–36] Moreover, the effects of notch root radius on the plane strain fracture toughness $K_{1C}(\rho)$ of Si_3N_4 and Al_2O_3 were well described using the process zone size failure criterion, as a function of σ_0 and K_{1C}.[34,36] In Fig. 6, a schematic relation between σ_C and a_e is shown to explain the relationship between proof stress and maximum residual equivalent crack size. The dotted line and solid line show the relationship between σ_C and a_e at room temperature and high temperature, respectively. If the proof test is made at room temperature, a maximum residual equivalent crack size a_e^R can be expressed as follows using Eq. (3);

$$a_e^R = \frac{\pi}{8}\left\{\frac{K_{1c}^R}{\sigma_0^R}\right\}^2\left\{\sec\left(\frac{\pi\sigma_P^R}{2\sigma_0^R}\right) - 1\right\}^{-1} \tag{4}$$

where, K_{1C}^R, σ_0^R and σ_P^R are the plane strain fracture toughness, the process zone forming stress (fracture stress of plain specimen) and the proof stress at room temperature, respectively.

Assuming that embedded flaws cannot be healed even at high temperature, then the maximum residual equivalent crack size a_e^R is not changed even at high temperature. The proof stress σ_P^T at high temperature T can be expressed as follows based on Eqs. (3) and (4).

$$\sigma_P^T = \frac{2\sigma_0^T}{\pi}\arccos\left\{\left[\left(\frac{K_{1c}^T}{K_{1c}^R}\right)^2\left(\frac{\sigma_0^R}{\sigma_0^T}\right)^2\left[\sec\frac{\pi\sigma_P^R}{2\sigma_0^R} - 1\right] + 1\right]^{-1}\right\} \tag{5}$$

where K_{1C}^T, σ_0^T and σ_P^T are the plane strain fracture toughness, the process zone forming stress (fracture stress of plain specimen) and the proof stress at high temperature T, respectively. σ_P^T is to be interpreted as the calculated minimum fracture stress for the high temperature service.

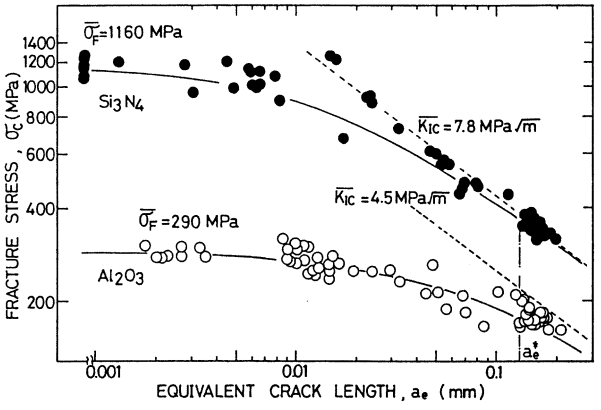

Fig. 5. Fracture stress versus equivalent crack length.

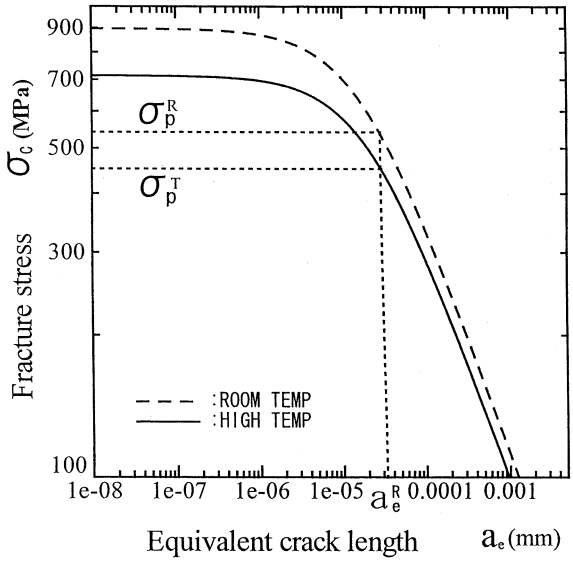

Fig. 6. The effect of equivalent crack length on fracture stress at room temperature and high temperature.

3. Materials, specimen and test method

The silicon nitride powder used in this investigation has the following properties: mean particle size = 0.2 μm, the volume ratio of α-Si_3N_4 is about 95% and the rest is β-Si_3N_4. The samples were made with a mixture of silicon nitride, 5 wt.% Y_2O_3 and 3 wt.% Al_2O_3 as an additive powder. To this mixture, alcohol was added. Subsequently, methyl cellulose, plasticizers and alcohol were added to the mixture as binders and solvent, respectively. The mixture was kneaded after mixing of the additives. After this process, the mixture was formed into a rod via an extruder. This is a raw material for a ceramics coil spring.[37] Then, the organic binders were burnt off. Subsequently, sintering was carried out in 0.93 MPa N_2 gas for 4 h at 1850°C. The sintered rod was then cut into test pieces measuring ϕ 2.4×40 mm. To measure K_{1C}, a three-point bend sample 3×4×40 mm were made. The relative density of K_{1C} and the rod is about 91%. A very sharp V notch was made on the K_{1C} sample and measured K_{1C}, where the v notch shape is: depth = 2 mm, notch angle = 45°, notch root radius = 0.1 mm. A cracked sample is not used because the

crack will be healed during heating up. It is shown that the cracked sample and notched sample showed almost the same fracture toughness, theoretically and experimentally, if the notch root radius is smaller than 0.2 mm.[36a]

Usually, a small bending sample is used to measure strength. The effective volume of such a sample is small. Then the probability that such a sample contains the very harmful embedded flaw is very low. However, if the effective volume of the component is large, even though the machine component is hot-pressed, the probability that such a component contains the very harmful embedded flaw is not low. To simulate this situation, many flaws were introduced on purpose in the rod and K_{1C} sample during the sintering process using a binder. Also, using pressureless sintering in N_2 environment, the disappearance or healing of the flaws during the sintering process was avoided intentionally. As mentioned before, even surface flaws cannot be healed in N_2 environment.

As a preliminary study, the best flaw-healing condition was investigated. It was shown that the best healing condition for this material in terms of static strength up to 1200°C is at a temperature of 1200∼1300°C with a healing time of 1 h in air. Some specimens were healed under these conditions (1200°C) before the proof test. Fig. 7 shows the surface condition of a sample before and after healing. There are many pores before healing, as shown in Fig. 7(a) and (b). These pores are tracks of burned organic binders. It is the purpose of healing to heal these pores so as to increase reliability. Fig. 7(c) shows the surface conditions after healing treatment. Most pores were healed completely. After healing treatment, X-ray analysis has been made to examine whether healed materials are crystal or not. It was found that most healing material was glassy phase.

All proof tests, fracture tests of rod sample and K_{1C} test were made on a three point loading system. The test system of the rod sample is shown schematically in Fig. 8. The cross-head speed in the tests was 0.5 mm/min. Proof tests were carried out at room temperature and the proof stress was 598 and 700 MPa.

4. Test result

4.1. Temperature dependence of K_{1C}, fracture strength σ_0^T and proof stress σ_P^T

The temperature dependence of the plane strain fracture toughness K_{1C} and fracture stress of plain specimen σ_0^T of bend specimen are shown in Fig. 9. K_{1C} is about 6 MPa$\sqrt{}$ m and is almost independent of temperature from room temperature to 1300°C. Fracture stress σ_0^T is determined as the average fracture stress of 10 crack-healed specimens which showed the highest fracture stress within about 40 specimens at each temperature. The σ_0^T is almost constant up to 1000°C. However, above 1100°C, σ_0^T decreases with increasing test temperature. This decreasing of σ_0^T at high temperature is

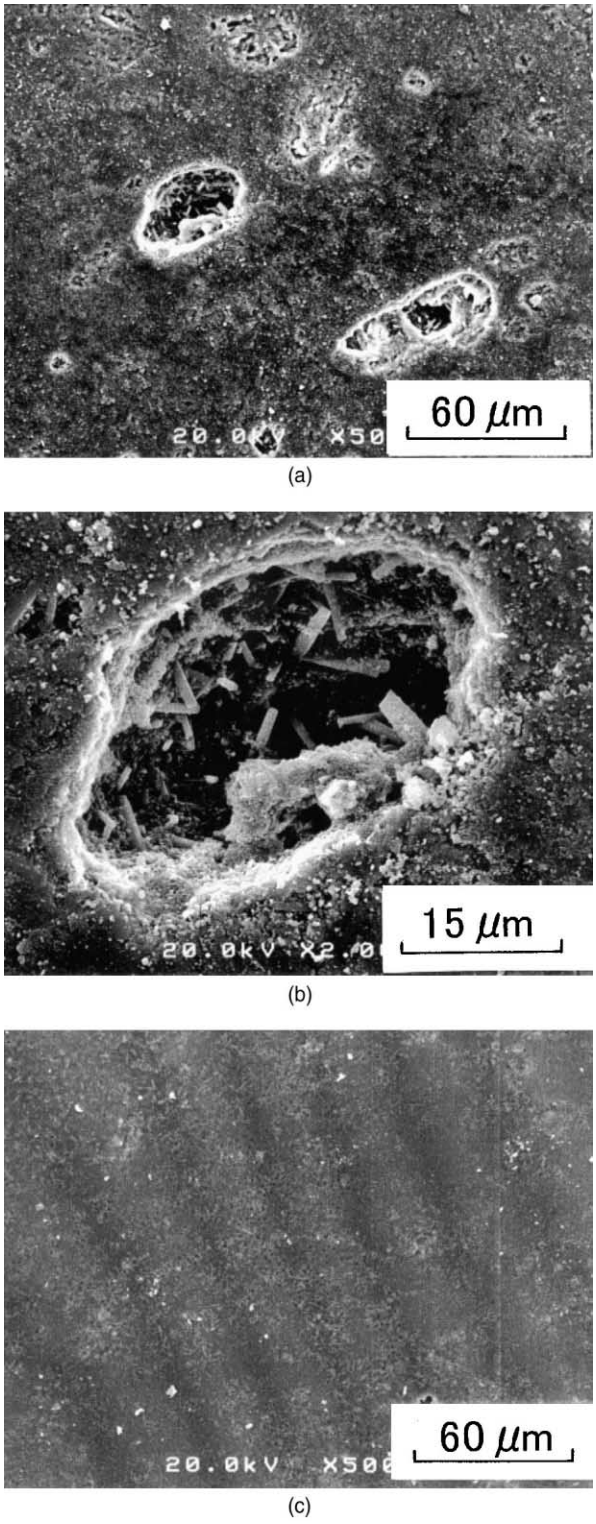

Fig. 7. Surface conditions of specimen after and before crack-healing: (a) before crack-healing; (b) in detail of (a); (c) after crack-healing.

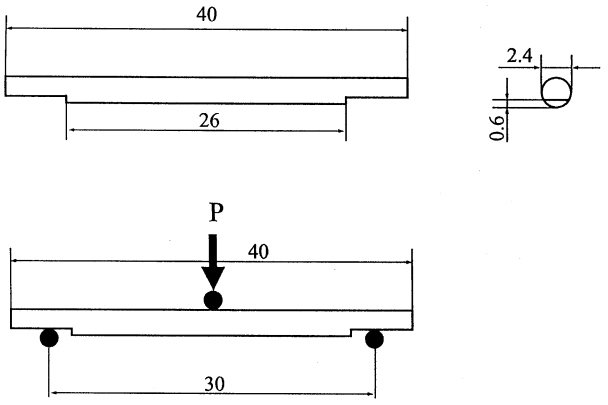

Fig. 8. Specimen and three-point bend test system.

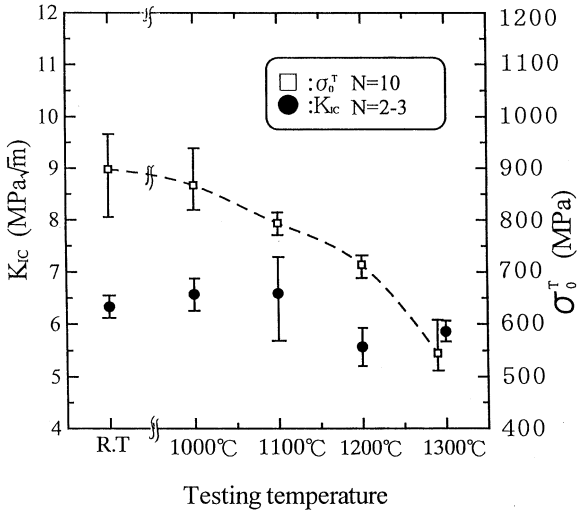

Fig. 9. The effect of test temperature on fracture stress σ_0 and plane strain fracture toughness K_{1C}.

caused by the fact that the grain boundary and healing material are not crystallized.

Temperature dependence of calculated proofed stress σ_P^T is shown in Fig.10 as a function of proof test stress at room temperature σ_P^R. From Eq. (3), it can be easily understood that the temperature dependence of σ_P^T is affected only by the temperature dependence of both σ_O^T and K_{1C}. The characteristic of temperature dependence of σ_P^T is divided into two cases, roughly. When σ_P^R is relatively large compared to σ_O^R ($\sigma_O^R > \sigma_P^R > 0.7\sigma_O^R$), temperature dependence of σ_P^T is mainly dependent on the temperature dependence of σ_O^T because a structural ceramics shows non-linear fracture behaviour as shown in Fig. 5. In contrast, when σ_P^R is small compared to σ_O^R ($\sigma_P^R \leqslant 0.5\sigma_O^R$), the temperature dependence of σ_P^T is mainly dependent on the temperature dependence of K_{1C} because fracture behaviour is controlled by K_{1C}. When σ_P^R is 700 or 598 MPa (Fig. 10) the above-mentioned first characteristic can be observed clearly: namely, σ_P^T decreases with increasing temperature similar to σ_O^R. In contrast, when σ_P^R is 417 MPa, σ_P^T shows just a little

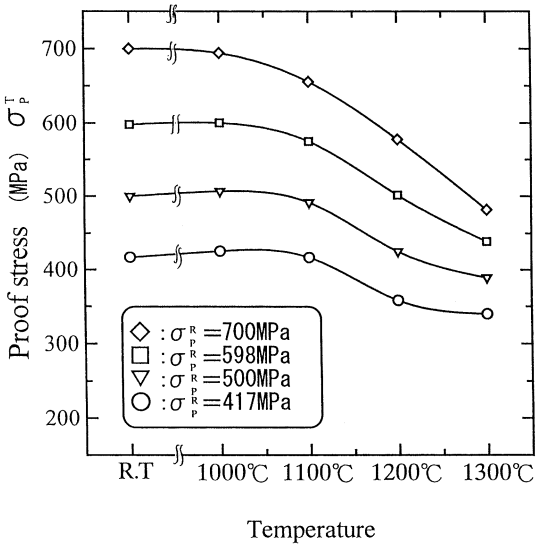

Fig. 10. Temperature dependence of calculated proof stress at high temperature as a function of proof test stress at room temperature.

temperature dependence. This behaviour is caused by the fact that temperature dependence of K_{1C} is slight.

4.2. Comparison between calculated minimum fracture stress (σ_P^T) and experimental fracture stress

In Fig. 11, comparison between the proof stress (calculated minimum fracture stress: σ_P^T) and the experimental fracture stress is shown. Fig. 11(a) shows the case where σ_P^R is 598 MPa for the rod sample. Symbol ○ shows the fracture stress of the as-received rod specimens, and □ shows the fracture stress of the crack-healed rod specimens. Symbols ● and ■ show the average value of the fracture stress of the as-received and crack-healed rod specimens, respectively. The lowest fracture stress of these specimens is almost the same value up to 1200°C and shows a little higher value than that of calculated minimum fracture stress (σ_P^T) at each temperature. By contrast, the lowest fracture stress of these specimens at 1300°C showed a lower value. However, the lowest fracture stress is 442 MPa and the calculated minimum fracture stress (σ_P^T) is 439 MPa. The experimental fracture stress is a little higher than that of the calculated σ_P^T.

Fig. 11(b) shows test data on rod specimen where σ_P^R is 700 MPa. The symbol □ shows the fracture stress of the crack-healed rod sample. The bend test has been made on 14 specimens at each temperature. The lowest fracture stress at 1100°C is 647 MPa and the calculated σ_P^T is 654 MPa. The experimental fracture stress of two specimens is a little lower than the calculated minimum fracture stress σ_P^T. At 1200°C, the lowest fracture stress is 532 MPa and the calculated σ_P^T is 580 MPa. Two samples showed a little lower fracture stress than calculated minimum fracture stress. For the case of high

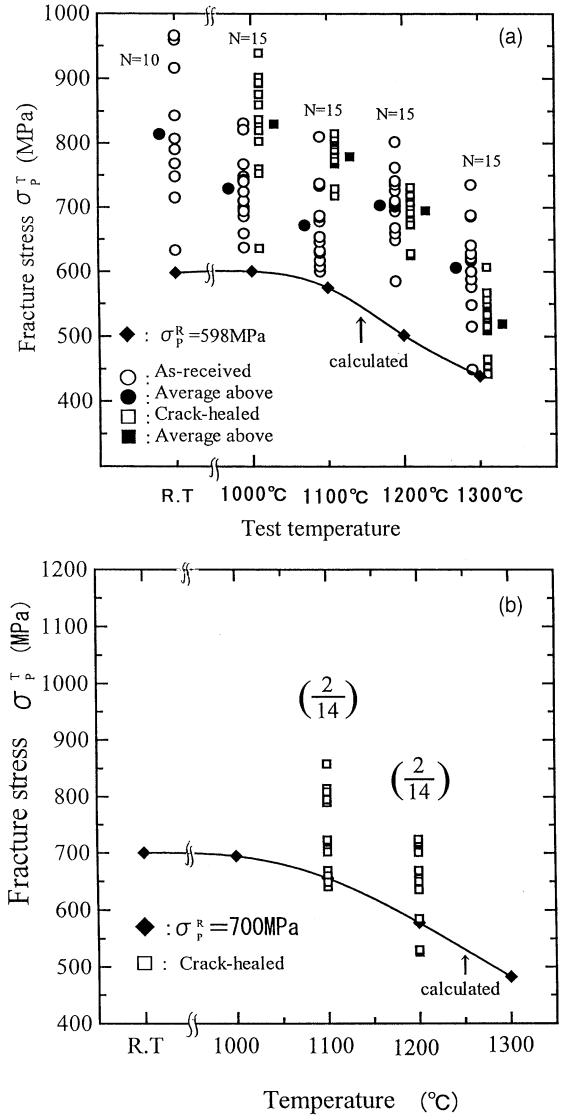

Fig. 11. The comparison between the calculated proof stress and experimented one as a function of test temperature and proof test stress: (a) proof test stress at room temperature is 598 MPa; (b) proof test stress at room temperature is 700 MPa.

proof stress, experimental minimum fracture stress is a little lower than the calculated one. This fact was assumed to occur by the fact that micro-structural flaws (such as abnormally large grain and weak grain boundary) were not taken into consideration. From the above two figures, generally speaking it can be concluded that the calculated minimum fracture stress provides a reliable lower limit to the fracture stress of the crack-healed and proof-tested specimens.

5. Conclusions

A new model and equation are proposed for the temperature-dependence of the proof stress of structural ceramics. Silicon nitride rod with many pores was sintered. This specimen was proof tested at room temperature and fracture tested at high temperature. A comparison between calculated minimum fracture stress and the experimental lowest fracture stress has been made to show the accuracy of the equation proposed. The main features of this work are as follows:

1. A new model and equation are proposed to show the temperature dependence of proof stress (minimum fracture stress), using the process zone size failure criterion by Ando[32,34].
2. The temperature dependence of the minimum fracture stress is calculated as a function of proof test stress at room temperature and testing temperature, using temperature dependence of K_{1C} and fracture stress of plain specimen σ_0. Measured fracture stresses of proof tested samples are consistently greater than the calculated minimum fracture stress in the high temperature range from 1000 to 1300°C.
3. From the abovementioned conclusions and the fact that crack-healed zone show excellent mechanical behaviour, it can be concluded that the technique (crack-healing + proof test) is a useful one to guarantee a reliability of structural ceramics components.

References

1. Lange, J. J. and Gupta, T. K., Crack-healing by heat treatment. *J. Am. Ceram. Soc.*, 1970, **53**, 54–55.
2. Lange, J. J. and Radford, K. C., Healing of surface cracks in polycrystalline Al_2O_3. *J. Am. Ceram. Soc.*, 1970, **53**, 420–421.
3. Petrovic, J. J. and Jacobson, L. A., Controlled surface flaws in hot-pressed SiC. *J. Am Ceram. Soc.*, 1976, **59**, 34–37.
4. Gupta, T. K., Crack-healing and strengthening of thermally shocked alumina. *J. Am Ceram. Soc.*, 1976, **59**, 259–262.
5. Choi, S. R. and Tikara, V., Crack-healing behavior of hot-pressed silicon nitride due to oxidation. *Scripta Metall. Mater.*, 1992, **26**, 1263–1268.
6. Chu, M. C., Sato, S., Kobayashi, Y. and Ando, K., Study on strengthening of mullite by dispersion of carbide ceramics particles. *Jpn. Soc. Mech. Eng.*, 1994, **60**(580A), 2829–2834 (in Japanese).
7. Chu, M. C., Sato, S., Kobayashi, Y. and Ando, K., Damage healing and strengthening behavior in intelligent mullite/SiC ceramics. *Fatigue Fract. Eng. Mater. Struct.*, 1995, **18**(9), 1019–1029.
8. Sato, S., Chu, M. C., Kobayashi, Y. and Ando, K., Strengthening of mullite by dispersion of carbide ceramics particles. *Jpn. Soc. Mech. Eng.*, 1995, **61**(585A), 1023–1030 (in Japanese).
9. Moffatt, J. E., Plumbridge, W. J. and Hermann, R., High temperature crack annealing effect on fracture toughness of alumina and alumina–SiC composite. *Bri. Ceram. Trans.*, 1996, **95**, 23–29.
10. Ando, K., Ikeda, T., Sato, S., Yao, F. and Kobayashi, Y., A preliminary study on crack healing behavior of Si3N4/SiC composite ceramics. *Fatigue Fract. Eng. Mater. Struct.*, 1998, **21**, 119–122.
11. Chu, M. C., Ando, K., Sato, S., Hirasawa, T. and Kobayashi, Y., Crack-healing behavior of silicon nitride ceramics(effect of chemical composition on crack healing ability). *High Pressure Inst. Jpn.*, 1998, **36–2**, 82–89 (in Japanese).
12. Ando, K., Chu, M. C., Sato, S., Yao, F. and Kobayashi, Y., The study on crack healing behavior of silicon nitride ceramics. *Jpn. Soc. Mech. Eng.*, 1998, **64**(623A), 1936–1942 (in Japanese).

13. Zhang, Y. Z., Edwards, L. and Plumbridge, W. J., Crack healing in a Silicon Nitride Ceramics. *J. Am. Ceram. Soc.*, 1998, **81**, 1861–1868.
14. Ando, K., Tsuji, K., Hirasawa, T., Kobayashi, Y., Chu, M. C. and Sato, S., Crack healing behavior and high temperature strength of mullite/SiC composite ceramics. *J. Soc. Mater. Sci. Jpn.*, 1999, **48**(5), 484–494 (in Japanese).
15. Ando, K., Tsuji, K., Ariga, M. and Sato, S., Fatigue strength properties of crack healed mullite/SiC composite ceramics. *J. Soc. Mater. Sci., Jpn*, 1999, **48**(10), 1173–1178.
16. Ando, K., Chu, M. C., Kobayashi, Y., Yao, F. and Sato, S., Crack healing behavior and high temperature strength of silicon nitride ceramics. *Jpn. Soc. Mech. Eng.*, 1999, **65**(633A), 1132–1139(in Japanese).
17. Ando, K., Chu, M. C., Yao, F. and Sato, S., Fatigue strength of crack-healed Si3N4/SiC composite ceramics. *Fatigue Fract. Eng. Mater. Struct.*, 1999, **22**, 897–903.
18. Yao, F., Ando, K., Chu, M. C. and Sato, S., Crack-healing behavior, high-temperature and fatigue strength of SiC-reinforced silicon nitride composite. *J. Mater. Sci. (Letts)*, 2000, **12**(19), 1081–1084.
19. Korous, Y., Chu, M. C., Nakatani, M. and Ando, K., Crack healing behavior of SiC ceramics. *J. Am. Ceram. Soc.*, 2000, **83**, 2788–2792.
20. Chu, M. C., Matsushita, S, Sato, S. and Ando, K., The low-cycle fatigue strength of crack-healed Si3N4/SiC composite ceramics. *J. Am. Ceram. Soc.*, (submitted for publication).
21. Ando, K., Tuji, K., Furusawa, K., Hanagata, T., Chu, M. C. and Sato, S., Effect of pre-crack size and testing temperature on fatigue strength properties of crack-healed mullite. *J. Soc. Mater. Sci. Jpn.*, 2001, **50**(8), 921–925.
22. Yao, F., Ando, K., Chu, M. C. and Sato, S., Static and cyclic behaviour of crack-healed Si3N4/SiC composite ceramics. *J. Euro. Ceram. Soc.*, 2001, **21**, 991–997.
23. Wiederhorn, S. M. and Tighe, N. J., Proof-testing of hot-pressed silicon nitride. *J. Mater. Sci.*, 1978, **13**, 1781–1793.
24. Ritter, J. E. Jr., Oates, P. B., Fuller, E. R. Jr. and Wiederhorn, S. M., Proof testing of ceramics (part 1 Experiment). *J. Mater. Sci.*, 1980, **15**, 2275–2281.
25. Ritter, J. E. Jr., Oates, P. B., Fuller, E. R. Jr. and Wiederhorn, S. M., Proof testing of ceramics (part 2 Theory). *J. Mater. Sci.*, 1980, **15**, 2282–2295.
26. Jakus, K., Service, T. and Ritter, J. E. Jr., High-temperature fatigue behavior of polycrystalline alumina. *J. Am. Ceram. Soc.*, 1980, **6**, 4–7.
27. Jakus, K., Fahey, J. P. and Ritter, J. E. Jr., Improving the reliability of hot-pressed silicon nitride. In *Fract. Mech. Ceram. 5*, ed. R. C. Bradt, A. G. Evans, D. P. H., Hasselman and F. F. Lange. Plenum Publishing Co., 1983, pp. 425–434.
28. Hoshide, T., Sato, T. and Inouem, T., Fatigue properties of ceramics after proof testing (1st report theoretical analysis). *Jpn. Soc. Mech. Eng.*, 1990, **56**(A), 212–218 (in Japanese).
29. Hoshide, T., Sato, T., Ohara, T. and Inoue, T., Fatigue properties of ceramics after proof testing (2nd report experimental study). *Jpn. Soc. Mech. Eng.*, 1990, **56**(A), 220–223 (in Japanese).
30. Ando, K., Sato, S., Sone, S. and Kobayashi, Y. Probabilistic study on fatigue life of proof tested ceramics spring. In *Fracture From Defects* (ECF-12), ed. M. W. Brown, E. R. de los Rios and K. J. Miller. EMAS. Publishing, 1998, pp. 569–574.
31. Ando, K., Sato, S., Kobayashi, Y. and Chu, M. C. Crack healing behaviour of Si_3N_4 ceramics and its application to structural integrity. In *Fracture From Defects* (ECF-12), ed. M. W. Brown, E. R. de los Rios and K. J. Miller. Engineering Materials Advisory Services, 1998, pp. 497–502.
32. Ando, K., Kim, B. A., Iwasa, M. and Ogura, N., Process zone size failure criterion and probabilistic fracture aassessment curves for ceramics. *Fatigue Fract. Eng. Mater. Struct.*, 1992, **15**(2), 139–149.
33. Dugdale, D. S., Yielding of steel sheets containing slits. *J. Mech. Phys. Solids.*, 1960, **8**, 100–104.
34. Ando, K., Iwasa, M., Kim, B. A., Chu, M. C. and Sato, S., Effect of crack length, notch root radius and grain size on fracture toughness of fine ceramics. *Fatigue Fract. Eng. Mater. Struct.*, 1993, **16**, 995–1006.
35. Chu, M. C. and Ando, K., A fracture and severity analysis of composite ceramics. *Fatigue Fract. Eng. Mater. Struct.*, 1993, **16**(3), 335–350.
36. Tuji, K., Iwase, K. and Ando, K., The location of crack initiation sites in alumina, polycarbonate and mild steel. *Fatigue Fract. Eng. Mater. Struct.*, 1999, **12**, 509–517.
37. Sato, S.Taguchi, K. Adachi, R. and Nakatani, M., A study on strength characteristics of Si_3N_4 coil spring. *Fatigue Fract. Eng. Mater. Struct.*, 1996, **19**, 529–537.